ACCOUNTS
of chemical research

Zeolite Thin Films: From Computer Chips to Space Stations

CHRISTOPHER M. LEW, RUI CAI, AND YUSHAN YAN*
Department of Chemical and Environmental Engineering, University of California, Riverside, California 92521

RECEIVED ON MAY 5, 2009

CONSPECTUS

Zeolites are a class of crystalline oxides that have uniform and molecular-sized pores (3−12 Å in diameter). Although natural zeolites were first discovered in 1756, significant commercial development did not begin until the 1950s when synthetic zeolites with high purity and controlled chemical composition became available. Since then, major commercial applications of zeolites have been limited to catalysis, adsorption, and ion exchange, all using zeolites in powder form. Although researchers have widely investigated zeolite thin films within the last 15 years, most of these studies were motivated by the potential application of these materials as separation membranes and membrane reactors. In the last decade, we have recognized and demonstrated that zeolite thin films can have new, diverse, and economically significant applications that others had not previously considered. In this Account, we highlight our work on the development of zeolite thin films as low-dielectric constant (low-*k*) insulators for future generation computer chips, environmentally benign corrosion-resistant coatings for aerospace alloys, and hydrophilic and microbiocidal coatings for gravity-independent water separation in space stations.

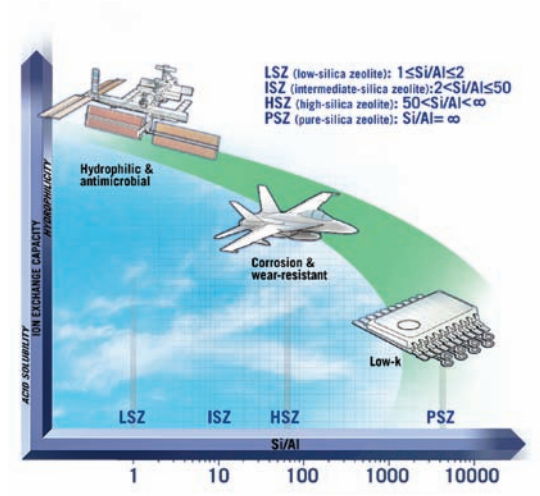

Although these three applications might not seem directly related, they all rely on the ability to fine-tune important macroscopic properties of zeolites by changing their ratio of silicon to aluminum. For example, pure-silica zeolites (PSZs, Si/Al = ∞) are hydrophobic, acid stable, and have no ion exchange capacity, while low-silica zeolites (LSZs, Si/Al < 2) are hydrophilic, acid soluble, and have a high ion exchange capacity. These new thin films also take advantage of some unique properties of zeolites that have not been exploited before, such as a higher elastic modulus, hardness, and heat conductivity than those of amorphous porous silicas, and microbiocidal capabilities derived from their ion exchange capacities.

Finally, we briefly discuss our more recent work on polycrystalline zeolite thin films as promising biocompatible coatings and environmentally benign wear-resistant and antifouling coatings. When zeolites are incorporated into polymer thin films in the form of nanocrystals, we also show that the resultant composite membranes can significantly improve the performance of reverse osmosis membranes for sea water desalination and proton exchange membrane fuel cells.

These diverse applications of zeolites have the potential to initiate new industries while revolutionizing existing ones with a potential economic impact that could extend into the hundreds of billions of dollars. We have licensed several of these inventions to companies with millions of dollars invested in their commercial development. We expect that other related technologies will be licensed in the near future.

1. Brief Introduction to Zeolite Structure

Zeolites are porous aluminosilicates consisting of tetrahedra linked together at the corners to form a three-dimensional network. The tetrahedra consist of a "T" atom at the center, such as Si or Al, bonded to four oxygen atoms at the corners. The tetrahedra are organized in such a way as to create over 191 currently known framework types, each with a

Published on the Web 10/23/2009 www.pubs.acs.org/acr
10.1021/ar900146w
© 2010 American Chemical Society

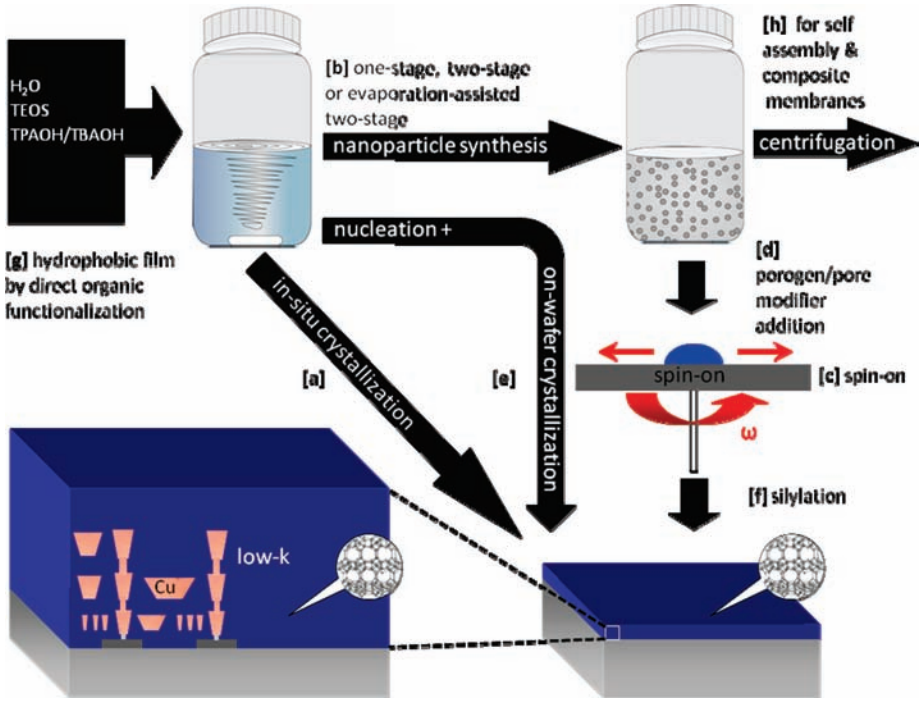

FIGURE 1. Schematic of the different film synthesis routes for PSZ low-*k* films and other films.[11,13,15,16,20,21,29−31,35−39,62−64]

unique topology and three-letter code assigned by the International Zeolite Association.[1] The zeolite channel and pore diameters are determined by the ring size, which is the number of T atoms bonded together (with oxygen atoms in-between each T atom) to form a ring. These pore openings consist of 6-, 8-, 9-, 10-, 12-, 14-, 18-, and 20-membered rings.

Since Si has a charge of 4+ and Al has a charge of 3+, the isomorphous substitution of Al for Si results in a negatively charged framework, which is compensated by cations such as Na^+ and K^+. This is the origin of the zeolites' ion exchange capacity. The Si/Al ratio can be changed from 1:1 to infinity when all zeolite framework types are considered, and this has a profound impact on their hydrophilicity, ion exchange capacity, and acid stability (Conspectus figure). Several texts give further details on zeolite structure and general introductory details.[2−4]

2. Low-Dielectric-Constant Films

As the feature sizes of next-generation microprocessors reach into the 32 nm node, the difficulty of finding a suitable dielectric interconnect material with a *k* value lower than 2.5 continues to slow down development along Moore's Law.[5] Amorphous porous silica and polymers have gained considerable research attention due to the low *k* value of air ($k \approx 1.0006$).[6−9] The mechanical integrity of these materials, however, is a concern because higher porosities generally result in poor mechanical strength, which is needed for survival during the chemical mechanical polishing processes.[10] (The elastic modulus is a common metric of mechanical stiffness, and the semiconductor industry generally requires a value of at least 6 GPa.[11]) With an intrinsic crystalline structure and uniform micropores, pure-silica zeolites (PSZs) offer several of the necessary properties for low-*k* applications,[8,12] including high porosity, mechanical strength, heat conductivity, thermal stability, and hydrophobicity. The films can be prepared through a manufacturing-friendly spin-on process of a zeolite nanoparticle suspension.[13] Furthermore, simple pre- and postsynthesis processing renders the films wet-etch chemical resistant with uniform mesopores.

Zeolite low-*k* films were first studied on PSZ MFI using an *in situ* deposition process (process [a] in Figure 1).[11] In this preparation method, a silicon substrate was submerged into a zeolite precursor solution, resulting in a uniform and *b*-oriented polycrystalline film (the *b* axis of the zeolite crystal was oriented perpendicular to the substrate). Transmission electron microscopy studies revealed that the crystals formed through a unique homogeneous nucleation process in the bulk solution and were subsequently deposited onto the substrate through self-assembly.[14] The *k* value and elastic modulus of the films were 2.7 and 30−40 GPa, respectively. However, this *in situ* crystallization process is considered impractical for low-*k* applications because of the risk associated with the immersion of the transistor-laden wafers in a corrosive synthesis solution. In addition, this method is a batch

process, which is against the established processing trend of single wafers in the semiconductor industry.

To be more manufacturing-friendly, a spin-on process was developed in which a PSZ MFI zeolite nanoparticle suspension was hydrothermally synthesized and then spun-on onto silicon wafers (processes [b] and [c] in Figure 1).[13] The suspension contained zeolite nanoparticles and aged amorphous silica precursors. The resultant zeolite films had a bimodal pore size distribution consisting of the intraparticle zeolite micropores and the interparticle mesopore void space, and consequently, the added mesoporosity lowered the *k* value and elastic modulus to 2.1 and 16−18 GPa, respectively. Additional mesoporosity could be added to the films through the addition of γ-cyclodextrin to the synthesized zeolite suspension (process [d] in Figure 1).[15] After a γ-cyclodextrin loading of 15%, the total porosity increased from 45% to 61% and the *k* value decreased to 1.8. The elastic modulus correspondingly decreased to 14.3 GPa, although this value is still significantly higher than the 6 GPa threshold value for low-*k* materials.

For spin-on zeolite films, nanoparticle suspensions with higher zeolite yield and crystallinity were found to decrease the *k* value.[16] For a one-stage synthesis method in which the synthesis solution is heated at one fixed temperature for a period of time, the typical way to obtain higher crystallinities is to increase the synthesis time. Unfortunately, longer synthesis times result in larger particles, which lead to unacceptably high film surface roughness and striations. To limit the crystal growth, space-confined synthesis strategies were developed using thermoreversible polymer gels[17] and reverse microemulsion coupled with microwave heating.[18] Adding methylene blue into the synthesis solution was also found to be effective in controlling the crystal growth.[19]

A more practical two-stage synthesis process was developed to keep the particle size small while increasing the yield and crystallinity by decoupling the nucleation from crystal growth (process [b] in Figure 1).[16] First, a low-temperature first stage focused on nuclei generation and was allowed to proceed for several days to maximize the number of nuclei. Then, the synthesis solution was abruptly brought to a high-temperature second stage that was maintained for several hours to allow for crystal growth. Through this method, a zeolite suspension with a yield of 76% and particle diameters less than 80 nm was achieved. In contrast, zeolite suspensions synthesized with a one-stage method with particles of 80 nm only had a yield of about 15%. The *k* value of the two-stage films decreased to 1.6. A further improvement in the *k* value was achieved by switching from an MFI-type zeolite with a framework density of 18.4 T atoms/nm^3 to an MEL-type zeolite with a framework density of 17.4 T atoms/nm^3.[20] By decreasing the framework density, the microporosity of the film increased, and thus, the *k* value decreased to 1.5. More recently, a new evaporation-assisted two-stage synthesis process (process [b] in Figure 1) was developed during which an evaporation step was added between the first and second stages.[21] Zeolite particles of bimodal size distribution with 98% of the particles at 14 nm in diameter and the rest at 60 nm were synthesized with a yield of 60%. Figure 2 shows how the zeolite particle size and yield change for different hydrothermal synthesis routes.

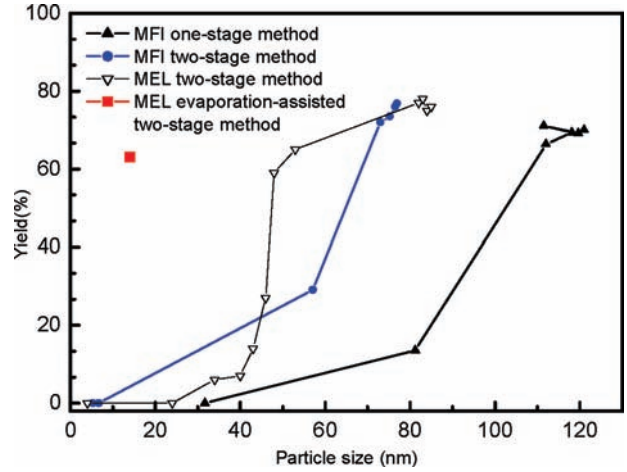

FIGURE 2. Particle size versus yield curves for different zeolite nanocrystal synthesis routes.[13,16,20,21]

While the evaporation-assisted films have a good combination of small particle size and high yield, a more preferable process would bypass the trade-off between these two properties altogether. An on-wafer crystallization method was developed to prepare zeolite low-*k* films in which the first-stage nucleated suspension (i.e., before crystal growth) is spun onto the silicon substrate (process [e] in Figure 1).[22] The substrate was then heated at ambient pressure to crystallize the film, and the final *k* and elastic modulus values were 1.8 and 16.8 GPa, respectively. Moreover, the film did not contain striations and had a surface roughness of $R_{rms} = 2.9$ nm. By crystallizing the zeolite films on-wafer, crystal sizes are kept to a minimum and features in the range of tens of nanometers are expected to be more easily patterned.

Nanoindentation measurements on polycrystalline zeolite films and spin-on films all reveal significantly higher elastic modulus values at any given *k* value over amorphous porous silica (Figure 3).[23−26] However, several fundamental questions need to be considered: (1) Does the substrate have an effect on the elastic modulus and hardness values of the thin films (<0.5 μm)? (2) Do intercrystalline grain boundaries in the poly-

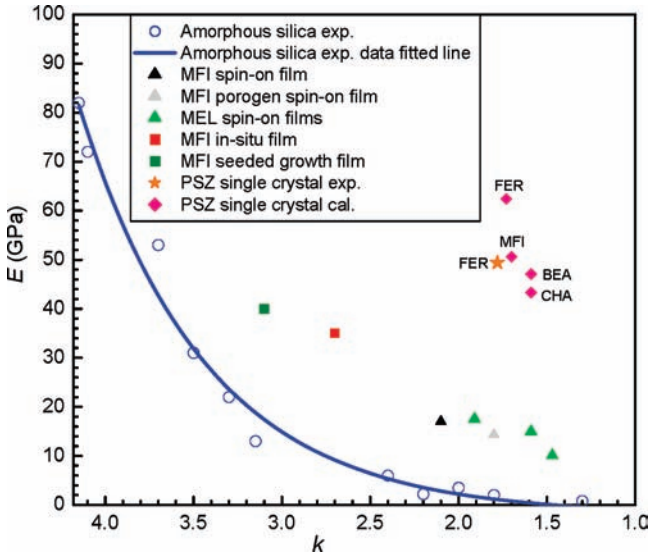

FIGURE 3. *E* versus *k* for zeolite films and crystals versus amorphous porous silica.[23] (Li, Z.; Johnson, M. C.; Sun, M.; Ryan, E. T.; Earl, D. J.; Maichen, W.; Martin, J. I.; Li, S.; Lew, C. M.; Wang, J.; Deem, M.; Davis, M. E.; Yan, Y. S. Mechanical and Dielectric Properties of Pure-Silica-Zeolite Low-k Materials. *Angew. Chem., Int. Ed.* **2006**, *45*, 6329−6332. Copyright Wiley-VCH Verlag GmbH & Co. KGaA. Reproduced with permission.)

crystalline films influence the properties? To answer these questions, large FER single crystals with a thin-plate geometry, an edge longer than 1 mm, and a thickness of about 30 μm were synthesized. These single crystals were free of substrate and intercrystalline grain boundaries. The resulting *k* and elastic modulus values were 1.8 and 49.4 GPa, respectively. Theoretical calculations were also performed on a number of pure-silica zeolites and confirmed that zeolite materials can have low *k* and high elastic modulus values (Figure 3). These results convincingly show that the elastic modulus measured on the thin films is reliable even though their thickness is about 500 nm, and that polycrystalline films have higher *k* and lower elastic modulus values than those of single crystals. Most importantly, this study confirms that the crystalline nature of the zeolites provides these films with their superior mechanical and dielectric properties.

Although initial studies on PSZ MFI showed that large crystals are intrinsically hydrophobic,[27] spin-on films have a large concentration of surface hydroxyl groups that render the films hydrophilic.[28] Since the *k* value of water is about 80, ambient moisture adsorption can increase the overall film dielectric constant to unacceptably high levels. Furthermore, the low-*k* materials are exposed to several corrosive wet-etch chemicals during the manufacturing process that can detrimentally degrade the films. Hydrofluoric acid (HF) is often used as a proxy for a chemical cleaning solution, and alternative low-*k* materials must demonstrate at least 5 min of HF resistance. To increase the films' hydrophobicity, vapor-phase silylation treatments with trimethylchlorosilane on PSZ low-*k* films were performed after annealing the films at 400 °C (process [f] in Figure 1).[13] Silanes have also been added to the zeolite precursor solution before synthesis in an effort to functionalize the zeolites with methyl or fluoroorganic groups (process [g] in Figure 1).[29,30] However, it was recently found that silylating the films after the annealing process, where substantial cross-linking of the amorphous silica matrix occurs, only resulted in surface silylation and poor HF resistance.[31] By introducing the uncalcined films to the silylation agent before the annealing step, more methyl groups were introduced into the amorphous silica matrix, and the films resisted HF for 5 min or more.

While higher porosity decreases the *k* value, large mesopores with a wide distribution in spin-on films can lead to poor pore sealing and nonuniform film properties.[32] Recent ellipsometric porosimetry (EP) measurements modeled the mesopore void space as ink bottle pores and revealed the existence of mesopores as wide as 35 nm.[33] Tetraethylorthosilicate (TEOS) can be added to the nanoparticle suspension before the spin-on process, and subsequent EP tests showed that the TEOS fills in the void spaces, resulting in a narrow pore size distribution with mesopores as small as 3.5 nm in diameter (process [d] in Figure 1). The pore size and porosity decreased as more TEOS was added.

The ability to pattern and control the zeolite structures may have uses in several electronic and optical applications.[34] Hierarchically patterned zeolite structures can be prepared by using zeolite nanocrystals as building blocks (discrete crystals from process [h] in Figure 1).[35−38] The specific techniques include soft-lithography, colloidal templating, and evaporation-assisted self-assembly. Furthermore, patterned zeolite structures can be created through a simple *in situ* crystallization process by taking advantage of the fact that zeolite films have poor adhesion to precious metals (process [a] in Figure 1).[39] A substrate was patterned with gold and placed into the synthesis solution, and the nucleated crystals self-assembled onto the areas without gold.

3. Chromium-Free Corrosion-Resistant Coatings

Metal corrosion is a ubiquitous problem and generally costs an industrialized country several percent of its gross domestic product (GDP) each year.[40,41] For aerospace applications, aluminum alloys are commonly used because they are light and mechanically strong, but some alloys have a high poten-

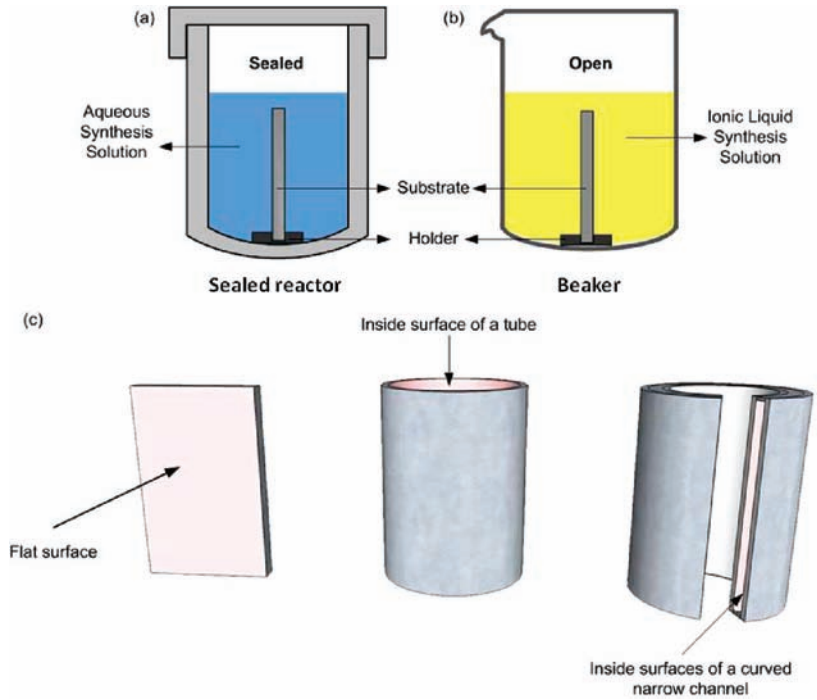

FIGURE 4. Schematics of (a) *in situ* crystallization process, (b) ambient pressure ionothermal synthesis process, and (c) examples of geometries that can be coated: a flat surface, the inside surface of a thin tube with an inner diameter of 3 mm, and the confined surface of a 3 mm wide-curved narrow channel.

tial for corrosion (e.g., Al-2024-T3). Chromate conversion coatings have been most durable and effective for protection of aerospace aluminum alloys, but their deposition process uses Cr^{6+}, which is a proven human carcinogen; thus, a chromium-free coating is preferred.[42]

Zeolites contain many of the properties necessary for a corrosion-resistant coating. The frameworks of high-silica and pure-silica zeolites (HSZs and PSZs) are extremely corrosion-resistant in pitting aggressive media and all mineral acids except hydrofluoric acid.[27] Furthermore, most HSZ and PSZ syntheses use an organic structure-directing agent (SDA) to form a specific framework, and after synthesis these SDA molecules remain in the zeolite pores. While catalysis and separation applications require the removal of the organic material by high temperature calcination, uncalcined and defect-free zeolite membranes are gastight.[43−45] Therefore, along with the chemical properties of the zeolite framework, the uncalcined membranes can physically block corrosive compounds and are strong candidates for chromium-free corrosion-resistant coatings.

Polycrystalline high-silica zeolite MFI coatings were synthesized on Al-2024-T3 through an *in situ* crystallization process (Figure 4a), and DC polarization tests showed that they were corrosion resistant in sulfuric acid and sodium hydroxide, media known for causing general corrosion.[46] They also performed remarkably well in neutral and acidified sodium chloride, which is known for causing pitting corrosion.[46] An added benefit of these coatings is that the *in situ* process can cover surfaces of complex shape and in confined spaces (e.g., non-line-of-sight surfaces, Figure 4c).

MTW, BEA, and MFI coatings were synthesized on different stainless steel and aluminum alloy substrates, and all were shown to be corrosion resistant, suggesting that corrosion resistance is general for all PSZs and HSZs.[47,48] After scaling the process up from small coupons (1 in. × 2 in.) to larger panels (3 in. × 6 in.), the coating deposition process was shown to be reproducible: out of the hundreds of panels produced, 99% passed the required corrosion resistance tests.[49] The coated panels were examined at the University of California, Riverside and military organizations with standard tests, including adhesion (ASTM D-3359), impact (ASTM D-2794), bending (ASTM D-552), salt-fog (ASTM B-117), and UV (ASTM G-154).[50] Additionally, the substrate pretreatment method consisted of a simple detergent washing process that was able to prepare all of the aluminum alloys and steels. More importantly, one general synthesis composition was developed to deposit high quality zeolite coatings on all aluminum alloys and steels.[51] Significant cost savings for the coating process were realized by unifying these processing conditions. Figure 5 contains scanning electron microscopy (SEM) images, digital photographs of zeolite-coated panels after 2000+ h in a

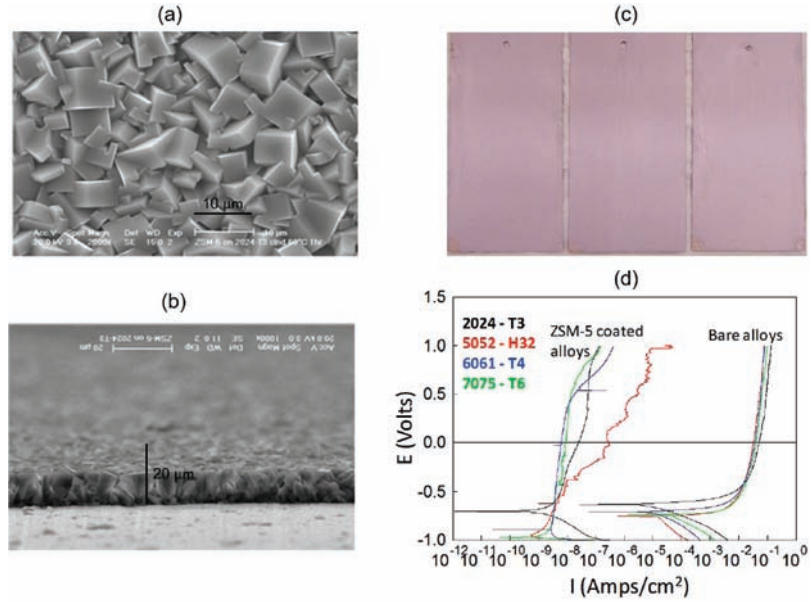

FIGURE 5. Experimental data on HSZ-MFI coatings on AA-2024-T3: (a) top-view SEM image, (b) cross-sectional SEM image, (c) digital photograph of coated 3 in. × 6 in. panels after 2000+ h salt-fog tests (ASTM B117), and (d) DC polarization test results in 0.5 M NaCl/HCl (pH 3.0).

salt-fog test, and DC polarization curves for zeolite corrosion-resistant coatings.

The *in situ* crystallization process occurs under autogenous pressure (9 atm at 175 °C), which is undesired by the surface-finishing industry. A more industry-friendly ambient pressure ionothermal synthesis was developed to prepare AlPO-11 and SAPO-11 (AEL-type framework) corrosion-resistant coatings under ambient pressures on aluminum alloys (Figure 4b).[52,53] Furthermore, ionic liquids are nonflammable and environmentally benign and should pose little threat to worker safety, and the microwave synthesis is simple and fast to operate. While the AlPO-11 coating had poor crystal intergrowth and was randomly oriented, the SAPO-11 coating was mostly *c*-oriented and had strong intergrowth. The SAPO-11 coating was shown by cross-sectional SEM imaging to consist of a porous top layer with a dense barrier layer underneath. After sealing the SAPO-11 coating with a layer of bis(triethoxysilyl)methane (BTSM) mixed with PSZ MEL nanocrystals, the BTSM-MEL-sealed SAPO-11 exhibited excellent anticorrosion properties. Work in the area of ionothermal synthesis as an alternative to hydrothermal synthesis is a focus of future research so that zeolite materials can be more industrially compatible.

4. Hydrophilic and Antimicrobial Coatings

In manned spacecraft, the temperature and humidity are controlled by condensers in the environmental control systems. The moisture-laden air normally condenses into small droplets that aggregate and are eventually driven out by gravity in terrestrial applications; however, the microgravity encountered in space causes the water droplets to remain entrained in the air flow systems, and these droplets are carried back to the cabin as foggy air or rain. Corrosion and bacteria growth can occur as a result of the condensation, and visibility can be difficult. Therefore, gravity-independent water separation is a key component for these condenser systems. The heat exchanger surfaces can be covered with hydrophilic zeolite coatings to change the condensation mode from dropwise to film-wise. Vacuum sipping can then be used to remove the water.[54−56] This process is shown schematically in Figure 6.

Low-silica, hydrophilic zeolite (LSZ) LTA coatings were prepared on stainless steel substrates by an *in situ* crystallization method.[54] Similar to the corrosion-resistant coatings, the *in situ* synthesis technique allows for a wide variety of surfaces to be coated, including those in confined spaces. The zeolite coatings were imparted with antimicrobial properties through silver ion-exchange. Incubation tests (0−24 h) revealed no surviving colony forming units (cfu), and 8 week and year-long durability tests showed that the coatings remained hydrophilic and antimicrobial after continuous immersion in water.[57]

The alkaline conditions that are commonly used in low-silica zeolite syntheses easily corrode several substrates, such as aluminum alloys. In order to remedy this situation, hybrid LTA/MFI coatings were prepared that were both hydrophilic and antimicrobial.[58] First, a high-silica zeolite MFI coating was synthesized on aluminum alloy. Low-silica zeolite LTA seed

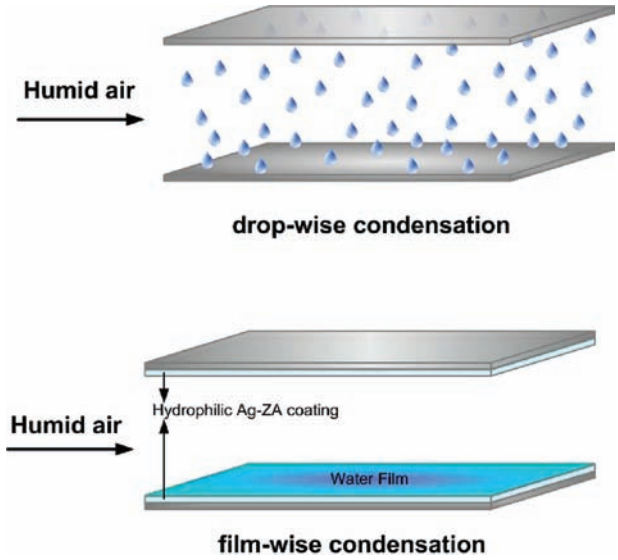

FIGURE 6. Schematic showing the condensation modes of uncoated and zeolite-coated heat exchanger surfaces for zero-gravity applications.

crystals between 200 and 500 nm were then dip-coated onto the MFI coating, and another short synthesis under the same conditions as the MFI base coating was performed. The resulting structure of zeolite LTA crystals embedded within an MFI matrix was silver ion-exchanged and had zero surviving cfu after *E. coli* incubation tests. Both the hybrid coatings and the zeolite LTA coatings on stainless steel exhibited excellent adhesion (average rating of 5B) from ASTM D-3359 cross-cut tape tests.

Limited heat transfer through the zeolite coatings was a concern because of their lower thermal conductivity over the metal substrates. However, under evaporating and condensing conditions, the hydrophilic coating allows for more spreading of the water droplets across the surface, which improves the heat transfer coefficient of the metal/coating system over the bare substrate.[59−61]

5. Future Directions

Zeolite nanocrystals (process [h] in Figure 1) can be incorporated into polymers, and the resulting composite membranes have shown improved performance for reverse osmosis and fuel cell membranes. Polycrystalline zeolite thin films have also been demonstrated to be promising as antifouling coatings, biocompatible coatings, and wear-resistant coatings.

As the world population continues to grow, clean and potable water is quickly becoming a scarce commodity, especially in dry regions. When zeolite nanoparticles were dispersed within polyamide reverse osmosis films, the flux doubled and salt rejections similar to commercially available membranes were maintained.[62] These improved membranes stand to dramatically improve the amount of available drinking water supplies at lower energy costs.

Nafion is the current standard proton exchange membrane (PEM) in PEM fuel cells. However, when methanol is used as the fuel, Nafion experiences a significant amount of methanol crossover that causes a loss of efficiency and mixed potential at the cathode. Moreover, Nafion loses its proton conductive properties at temperatures higher than 100 °C, which is the desired temperature regime for increased cathode kinetics. Composite membranes that have acid-functionalized zeolite nanoparticles embedded within the Nafion membrane have been shown to retain higher amounts of water, reduce the methanol crossover, and maintain similar levels of proton conductivity.[63−65] Overall higher performances of PEM fuel cells through the use of polymer/zeolite composite membranes can help to accelerate the commercial adoption of fuel cells as energy storage devices for a wide range of uses.

Biofouling and the deposition of microbes in aquatic environments seriously compromises military and industrial equipment by increasing hydrodynamic drag and clogging pipes, membranes, and filters. Billions of dollars are spent annually to counter these effects, and significant savings can be incurred by initial investments in prevention methods. LSZ LTA and HSZ MFI coatings were investigated for their biofouling properties.[66] Aluminum and stainless steel were coated with zeolite LTA and MFI, respectively, and bacterial transfer using a common marine bacterium, *Halomonas pacifica* g, was conducted in a parallel plate flow chamber system under laminar flow conditions. Both of the zeolite coatings had lower attachment efficiencies of *H. pacifica* g than the bare substrates. Moreover, the cell adhesion to the zeolite LTA coating, which was more hydrophilic, was less than that to the MFI coating. The combination of higher electrostatic repulsion and higher hydrophilicity for the zeolite coatings over the bare metals was the main factor in the reduced biofouling effects.

HSZ MFI coatings on titanium and titanium alloy were also shown to be corrosion resistant and biocompatible, thus showing excellent promise as coatings for biomedical implants.[67] Titanium alloy, Ti_6Al_4V, is commonly used for orthopedic and dental implants. However, it releases Al and V ions, which are toxic, and its elastic modulus (~110 GPa) does not match that of bone (10−40 GPa). As a result, implants often become loose and deosteointegrate. An MFI coating on titanium alloy was shown to be corrosion resistant and prevented the release of Al and V over 7 day tests

in highly acidic conditions. Furthermore, high cell adhesion and proliferation of pluripotent mouse embryonic stem cells was shown on the zeolite surface. With an elastic modulus similar to that of bone, the zeolite coatings are an ideal biocompatible coating for medical implants. (As opposed to the biofouling coatings, high cell adhesion for the biocompatible coatings was promoted under static conditions and biomineralization. The flowing conditions in normal marine environments cause low cell adhesion on zeolite coatings.)

Alternatives to cadmium and chromium wear-resistant coatings are preferred because the cadmium and chromium electroplating process uses carcinogenic and environmentally hazardous chemicals. MFI coatings were synthesized on stainless steel substrates, and the mechanical properties were compared to commercial electroplated cadmium and chromium coatings. Superior wear-resistance, as characterized by higher hardness values and shallower depths during nanoscratch tests, was shown for MFI coatings over cadmium coatings and chromium coatings in most of the practical high-wear applications. Moreover, stronger flexibility, resilience, and elastic recovery were exhibited by the MFI coatings, which are important in preventing crack formation during substrate bending and torsion. Finally, MFI coatings showed the best corrosion resistance during DC polarization tests, which indicated that zeolite coatings are superior alternative wear- and corrosion-resistant coatings.

6. Conclusions

We have shown that zeolites in a thin film form can have new, diverse, and significant commercial opportunities far beyond their traditional uses in catalysis, separation, and detergents. Zeolite thin films inherently possess the material properties necessary for new low-*k* materials, and future work is focused on reducing crystalline domain sizes to enable patterning of nanosized features. Zeolite coatings have also shown corrosion-resistance, and new synthesis techniques are currently under development to simplify the preparation of these coatings and develop ambient pressure processes that are fast, simple, and more economical. The most preferable method would be a spray-on method. Hydrophilic and antimicrobial zeolite coatings are excellent for covering the surfaces of heat exchangers in zero-gravity environments. New applications of zeolites, including reverse osmosis membranes, fuel cell membranes, antibiofouling coatings, biocompatible coatings, and wear-resistant coatings, continue to be explored and hold great promise for commercialization.

By utilizing properties that are inherent to zeolites, such as uniform porosity and ion exchange capabilities, zeolites have the potential to be useful to a wide variety of nontraditional applications. These new applications rely on identifying the critical needs of several fields that are usually considered unrelated to zeolites. Interestingly, these applications do not require the synthesis of new sophisticated framework structures. Most importantly, these new applications have significant implications for air, water, mobility, communication, and energy—the critical elements for a sustainable civilization.

We are thankful for the contributions from all of the Yan group members whose names appear in the references, and acknowledge the financial support from a large number of federal and state funding agencies and companies.

BIOGRAPHICAL INFORMATION

Christopher M. Lew received his B.S. and M.S. degrees from Stanford University in 2003, and his Ph.D. from the University of California at Riverside (UCR) in 2008. He is currently a postdoctoral scholar at UCR and is studying new materials for alternative energy applications.

Rui Cai received his B.S. degree from Nanjing University, China in 1999 and his Ph.D. from Dalian Institute of Chemical Physics, Chinese Academy of Sciences in 2005. He is currently a postdoctoral scholar at UCR and is interested in the synthesis and applications of zeolite nanocrystals and thin films.

Yushan Yan received his B.S. in Chemical Physics from the University of Science and Technology of China in 1988, and his M.S. and Ph.D. in Chemical Engineering from the California Institute of Technology in 1995 and 1997, respectively. He worked for AlliedSignal Inc. as a Senior Staff Engineer and Project Manager from 1996 to 1998. He joined UCR in 1998 as Assistant Professor and was promoted to Associate Professor in 2002 and Professor in 2005. He is currently the Department Chair. His research focuses on zeolite thin films and new materials for cheaper and more durable fuel cells.

FOOTNOTES

*To whom correspondence should be addressed. E-mail: Yushan.Yan@ucr.edu.

REFERENCES

1 Database of Zeolite Structures, http://www.iza-structure.org/databases/, International Zeolite Association (accessed January 17, 2009).

2 Breck, D. W. *Zeolite molecular sieves: structure, chemistry, and use*; John Wiley & Sons, Inc.: New York, 1973.

3 Dyer, A. *An Introduction to Zeolite Molecular Sieves*; John Wiley & Sons, Inc.: New York, 1988.

4 Xu, R.; Pang, W.; Yu, J.; Huo, Q.; Chen, J. *Chemistry of zeolites and related porous materials: synthesis and structure*; John Wiley & Sons, Inc.: Hoboken, NJ, 2007.

5 *International Technology Roadmap for Semiconductors*, 2007 edition; Interconnect: 2007, http://www.itrs.net/Links/2007ITRS/Home2007.htm (accessed on January 17, 2009).

6 Hrubesh, L. W. Aerogel applications. *J. Non-Cryst. Solids* **1998**, *225*, 335–342.

7 Hrubesh, L. W.; Keene, L. E.; Latorre, V. R. Dielectric-Properties of Aerogels. *J. Mater. Res.* **1993**, *8*, 1736–1741.

8 Maex, K.; Baklanov, M. R.; Shamiryan, D.; Iacopi, F.; Brongersma, S. H.; Yanovitskaya, Z. S. Low dielectric constant materials for microelectronics. *J. Appl. Phys.* **2003**, *93*, 8793–8841.

9 Seraji, S.; Wu, Y.; Jewell-Larson, N. E.; Forbess, M. J.; Limmer, S. J.; Chou, T. P.; Cao, G. Z. Patterned microstructure of sol-gel derived complex oxides using soft lithography. *Adv. Mater.* **2000**, *12*, 1421–1424.

10 Xu, G.; He, J.; Andideh, E.; Bielefeld, J.; Scherban, T. *Cohesive Strength Characterization of Brittle Low-k Films*. Proceedings of the IEEE International Interconnect Technology Conference, San Francisco, CA; Institute of Electrical and Electronics Engineers, 2002; pp 57−59.

11 Wang, Z. B.; Wang, H. T.; Mitra, A.; Huang, L. M.; Yan, Y. S. Pure-silica zeolite low-k dielectric thin films. *Adv. Mater.* **2001**, *13*, 746–749.

12 Morgen, M.; Ryan, E. T.; Zhao, J. H.; Hu, C.; Cho, T. H.; Ho, P. S. Low dielectric constant materials for ULSI interconnects. *Annu. Rev. Mater. Sci.* **2000**, *30*, 645–680.

13 Wang, Z. B.; Mitra, A. P.; Wang, H. T.; Huang, L. M.; Yan, Y. S. Pure silica zeolite films as low-k dielectrics by spin-on of nanoparticle suspensions. *Adv. Mater.* **2001**, *13*, 1463–1466.

14 Li, S.; Li, Z. J.; Bozhilov, K. N.; Chen, Z. W.; Yan, Y. S. TEM investigation of formation mechanism of monocrystal-thick b-oriented pure silica zeolite MFI film. *J. Am. Chem. Soc.* **2004**, *126*, 10732–10737.

15 Li, S.; Li, Z. J.; Yan, Y. S. Ultra-low-k pure-silica zeolite MFI films using cyclodextrin as porogen. *Adv. Mater.* **2003**, *15*, 1528–1531.

16 Li, Z. J.; Li, S.; Luo, H. M.; Yan, Y. S. Effects of crystallinity in spin-on pure-silica-zeolite MFI low-dielectric-constant films. *Adv. Funct. Mater.* **2004**, *14*, 1019–1024.

17 Wang, H. T.; Holmberg, B. A.; Yan, Y. S. Synthesis of template-free zeolite nanocrystals by using in situ thermoreversible polymer hydrogels. *J. Am. Chem. Soc.* **2003**, *125*, 9928–9929.

18 Chen, Z. W.; Li, S.; Yan, Y. S. Synthesis of template-free zeolite nanocrystals by reverse microemulsion-microwave method. *Chem. Mater.* **2005**, *17*, 2262–2266.

19 Lew, C. M.; Li, Z. J.; Zones, S. I.; Sun, M. W.; Yan, Y. S. Control of size and yield of pure-silica-zeolite MFI nanocrystals by addition of methylene blue to the synthesis solution. *Microporous Mesoporous Mater.* **2007**, *105*, 10–14.

20 Li, Z. J.; Lew, C. M.; Li, S.; Medina, D. I.; Yan, Y. S. Pure-silica-zeolite MEL low-k films from nanoparticle suspensions. *J. Phys. Chem. B* **2005**, *109*, 8652–8658.

21 Liu, Y.; Sun, M. W.; Lew, C. M.; Wang, J. L.; Yan, Y. S. MEL-type Pure-Silica Zeolite Nanocrystals Prepared by an Evaporation-Assisted Two-Stage Synthesis Method as Ultra-Low-*k* Materials. *Adv. Funct. Mater.* **2008**, *18*, 1732–1738.

22 Liu, Y.; Lew, C. M.; Sun, M. W.; Cai, R.; Wang, J.; Kloster, G. M.; Boyanov, B.; Yan, Y. S. On-Wafer Crystallization of Ultralow-k Pure Silica Zeolite Films. *Angew. Chem., Int. Ed.* **2009**, *48*, 4777–4780.

23 Li, Z. J.; Johnson, M. C.; Sun, M. W.; Ryan, E. T.; Earl, D. J.; Maichen, W.; Martin, J. I.; Li, S.; Lew, C. M.; Wang, J.; Deem, M. W.; Davis, M. E.; Yan, Y. S. Mechanical and dielectric properties of pure-silica-zeolite low-k materials. *Angew. Chem., Int. Ed.* **2006**, *45*, 6329–6332.

24 Johnson, M.; Li, Z. J.; Wang, J. L.; Yan, Y. S. Mechanical characterization of zeolite low dielectric constant thin films by nanoindentation. *Thin Solid Films* **2007**, *515*, 3164–3170.

25 Johnson, M. C.; Wang, J. L.; Li, Z. J.; Lew, C. M.; Yan, Y. S. Effect of Calcination and Polycrystallinity on Mechanical Properties of Nanoporous MFI Zeolites. *Mater. Sci. Eng., A* **2007**, *456*, 58–63.

26 Johnson, M. C.; Lew, C. M.; Yan, Y. S.; Wang, J. L. Hydrophobicity-dependent friction and wear of spin-on zeolite thin films. *Scr. Mater.* **2008**, *58*, 41–44.

27 Flanigen, E. M.; Bennett, J. M.; Grose, R. W.; Cohen, J. P.; Patton, R. L.; Kirchner, R. M.; Smith, J. V. Silicalite, a New Hydrophobic Crystalline Silica Molecular-Sieve. *Nature* **1978**, *271*, 512–516.

28 Li, S.; Wang, X.; Beving, D.; Chen, Z. W.; Yan, Y. S. Molecular sieving in a nanoporous b-oriented pure-silica-zeolite MFI monocrystal film. *J. Am. Chem. Soc.* **2004**, *126*, 4122–4123.

29 Lew, C. M.; Li, Z. J.; Li, S.; Hwang, S. J.; Liu, Y.; Medina, D. I.; Sun, M. W.; Wang, J. L.; Davis, M. E.; Yan, Y. S. Pure-silica-zeolite MFI and MEL low-dielectric constant films with fluoroorganic functionalization. *Adv. Funct. Mater.* **2008**, *18*, 3454–3460.

30 Li, S.; Li, Z. J.; Medina, D.; Lew, C.; Yan, Y. S. Organic-functionalized pure-silica-zeolite MFI low-k films. *Chem. Mater.* **2005**, *17*, 1851–1854.

31 Lew, C. M.; Liu, Y.; Day, B.; Kloster, G. M.; Tiznado, H.; Sun, M. W.; Zaera, F.; Wang, J.; Yan, Y. S. Hydrofluoric Acid-Resistant & Hydrophobic Pure-Silica-Zeolite MEL Low-Dielectric Constant Films. *Langmuir* **2009**, *25*, 5039–5044.

32 Dubois, G.; Miller, R. D.; Volksen, W. In *Dielectric Films for Advanced Microelectronics*; Baklanov, M. R., Green, M., Maex, K., Eds.; John Wiley and Sons, Ltd.: Great Britain, 2007; pp 33−83.

33 Eslava, S.; Baklanov, M. R.; Neimark, A. V.; Iacopi, F.; Kirschhock, C. E. A.; Maex, K.; Martens, J. A. Evidence of large voids in pure-silica-zeolite low-k dielectrics synthesized by spin-on of nanoparticle suspensions. *Adv. Mater.* **2008**, *20*, 3110–3116.

34 Davis, M. E. Ordered porous materials for emerging applications. *Nature* **2002**, *417*, 813–821.

35 Huang, L. M.; Wang, Z. B.; Sun, J. Y.; Miao, L.; Li, Q. Z.; Yan, Y. S.; Zhao, D. Y. Fabrication of ordered porous structures by self-assembly of zeolite nanocrystals. *J. Am. Chem. Soc.* **2000**, *122*, 3530–3531.

36 Huang, L. M.; Wang, Z. B.; Wang, H. T.; Sun, J. Y.; Li, Q. H.; Zhao, D. Y.; Yan, Y. S. Hierarchical porous structures by using zeolite nanocrystals as building blocks. *Microporous Mesoporous Mater.* **2001**, *48*, 73–78.

37 Wang, H. T.; Huang, L. M.; Wang, Z. B.; Mitra, A.; Yan, Y. S. Hierarchical zeolite structures with designed shape by gel-casting of colloidal nanocrystal suspensions. *Chem. Commun.* **2001**, 1364–1365.

38 Wang, H. T.; Wang, Z. B.; Huang, L. M.; Mitra, A.; Yan, Y. S. Surface patterned porous films by convection-assisted dynamic self-assembly of zeolite nanoparticles. *Langmuir* **2001**, *17*, 2572–2574.

39 Li, S.; Demmelmaier, C.; Itkis, M.; Liu, Z. M.; Haddon, R. C.; Yan, Y. S. Micropatterned oriented zeolite monolayer films by direct in situ crystallization. *Chem. Mater.* **2003**, *15*, 2687–2689.

40 Burstein, G. T. Metallurgy - Revealing Corrosion Pits. *Nature* **1991**, *350*, 188−189.

41 Newman, R. C.; Sieradzki, K. Metallic Corrosion. *Science* **1994**, *263*, 1708−1709.

42 Rabbetts, A. Replacements for hexavalent chromium in anodising and conversion coating. *Trans. Inst. Met. Finish.* **1998**, *76*, B4–B5.

43 Lin, X.; Falconer, J. L.; Noble, R. D. Parallel pathways for transport in ZSM-5 zeolite membranes. *Chem. Mater.* **1998**, *10*, 3716–3723.

44 Vroon, Z. A. E. P.; Keizer, K.; Burggraaf, A. J.; Verweij, H. Preparation and characterization of thin zeolite MFI membranes on porous supports. *J. Membr. Sci.* **1998**, *144*, 65–76.

45 Yan, Y. S.; Davis, M. E.; Gavalas, G. R. Preparation of Zeolite ZSM-5 Membranes by in-Situ Crystallization on Porous Alpha-Al_2O_3. *Ind. Eng. Chem. Res.* **1995**, *34*, 1652–1661.

46 Cheng, X. L.; Wang, Z. B.; Yan, Y. S. Corrosion-resistant zeolite coatings by in situ crystallization. *Electrochem. Solid-State Lett.* **2001**, *4*, B23–B26.

47 Mitra, A.; Kirby, C. W.; Wang, Z. B.; Huang, L. M.; Wang, H. T.; Huang, Y. N.; Yan, Y. S. Synthesis of pure-silica MTW powder and supported films. *Microporous Mesoporous Mater.* **2002**, *54*, 175–186.

48 Mitra, A.; Wang, Z. B.; Cao, T. G.; Wang, H. T.; Huang, L. M.; Yan, Y. S. Synthesis and corrosion resistance of high-silica zeolite MTW, BEA, and MFI coatings on steel and aluminum. *J. Electrochem. Soc.* **2002**, *149*, B472–B478.

49 Beving, D.; O'Neill, C.; Yan, Y. In *Studies in Surface Science and Catalysis*; Xu, R., Gao, Z., Chen, J., Yan, W., Eds.; Elsevier: Amsterdam, 2007; Vol. 170B; pp 1629−1636.

50 Beving, D. E.; Anderson, N.; O'Neill, C.; Yan, Y. Salt fog accelerated weathering testing of high-silica zeolite MFI coatings on aluminum alloy 2024-T3. *ECS Trans.* **2006**, *1*, 65–72.

51 Beving, D. E.; McDonnell, A. M. P.; Yang, W. S.; Yan, Y. S. Corrosion resistant high-silica-zeolite MFI coating - One general solution formulation for aluminum alloy AA-2024-T3, AA-5052-H32, AA-6061-T4, and AA-7075-T6. *J. Electrochem. Soc.* **2006**, *153*, B325–B329.

52 Cai, R.; Sun, M. W.; Chen, Z. W.; Munoz, R.; O'Neill, C.; Beving, D. E.; Yan, Y. S. Ionothermal synthesis of oriented zeolite AEL films and their application as corrosion-resistant coatings. *Angew. Chem., Int. Ed.* **2008**, *47*, 525−528.

53 Cai, R.; Yan, Y. Corrosion-resistant zeolite coatings. *Corrosion* **2008**, *64*, 271–278.

54 McDonnell, A. M. P.; Beving, D.; Wang, A. J.; Chen, W.; Yan, Y. S. Hydrophilic and antimicrobial zeolite coatings for gravity-independent water separation. *Adv. Funct. Mater.* **2005**, *15*, 336–340.

55 Yan, Y. Hydrophilic zeolite coatings. U.S. Patent 6,500,490, 2002.

56 Yan, Y. Hydrophilic zeolite coating. U.S. Patent 6,849,568, 2005.

57 O'Neill, C.; Beving, D. E.; Chen, W.; Yan, Y. S. Durability of hydrophilic and antimicrobial zeolite coatings under water immersion. *AIChE J.* **2006**, *52*, 1157–1161.

58 Beving, D. E.; O'Neill, C. R.; Yan, Y. S. Hydrophilic and antimicrobial low-silica-zeolite LTA and high-silica-zeolite MFI hybrid coatings on aluminum alloys. *Microporous Mesoporous Mater.* **2008**, *108*, 77–85.

59 Liu, J.; Aguilar, G.; Munoz, R.; Yan, Y. Hydrophilic zeolite coatings for improved heat transfer: A quantitative analysis. *AIChE J.* **2008**, *54*, 779–790.

60 Munoz, R.; Beving, D.; Mao, Y. C.; Yan, Y. S. Zeolite Y coatings on Al-2024-T3 substrate by a three-step synthesis method. *Microporous Mesoporous Mater.* **2005**, *86*, 243–248.

61 Munoz, R. A.; Beving, D.; Yan, Y. S. Hydrophilic zeolite coatings for improved heat transfer. *Ind. Eng. Chem. Res.* **2005**, *44*, 4310–4315.

62 Jeong, B. H.; Hoek, E. M. V.; Yan, Y. S.; Subramani, A.; Huang, X. F.; Hurwitz, G.; Ghosh, A. K.; Jawor, A. Interfacial polymerization of thin film nanocomposites: A new concept for reverse osmosis membranes. *J. Membr. Sci.* **2007**, *294*, 1–7.

63 Chen, Z. W.; Holmberg, B.; Li, W. Z.; Wang, X.; Deng, W. Q.; Munoz, R.; Yan, Y. S. Nafion/zeolite nanocomposite membrane by in situ crystallization for a direct methanol fuel cell. *Chem. Mater.* **2006**, *18*, 5669–5675.

64 Holmberg, B. A.; Hwang, S. J.; Davis, M. E.; Yan, Y. S. Synthesis and proton conductivity of sulfonic acid functionalized zeolite BEA nanocrystals. *Microporous Mesoporous Mater.* **2005**, *80*, 347–356.

65 Holmberg, B. A.; Wang, X.; Yan, Y. S. Nanocomposite Fuel cell membranes based on nafion and acid functionalized zeolite beta nanocrystals. *J. Membr. Sci.* **2008**, *320*, 86–92.

66 Chen, G. X.; Bedi, R.; Yan, Y. S.; Walker, S. L. Initial Bacterial Deposition on Bare and Zeolite-Coated Aluminum Alloy and Stainless Steel. *Langmuir* **2009**, *25*, 1620–1626.

67 Bedi, R. S.; Beving, D. E.; Zanello, L. P.; Yan, Y. S. Biocompatibility of Corrosion-Resistant Zeolite Coatings for Titanium Alloy Biomedical Implants. *Acta Biomater.* **2009**, *5*, 3265–3271.